Sterile neutrino dark matter from right-handed neutrino oscillations

Kenji Kadota and Kunio Kaneta
Center for Theoretical Physics of the Universe, Institute for Basic Science (IBS), Daejeon 34051, Korea

(Received 24 February 2017; published 13 June 2018)

We study a scenario where sterile neutrino (either warm or cold) dark matter (DM) is produced through (nonresonant) oscillations among right-handed neutrinos (RHNs) and can constitute the whole DM in the Universe, in contrast to the conventional sterile neutrino production through its mixing with the left-handed neutrinos. The lightest RHN can be sterile neutrino DM whose mixing with left-handed neutrinos is sufficiently small while heavier RHNs can have non-negligible mixings with left-handed neutrinos to explain the neutrino masses by the seesaw mechanism. We also demonstrate that, in our scenario, the production of sterile RHN DM from the decay of a heavier RHN is subdominant compared with the RHN oscillation production due to the x-ray and small-scale structure constraints.

DOI: 10.1103/PhysRevD.97.115021

I. INTRODUCTION

While it has been established that neutrinos are massive due to the discovery of neutrino oscillations [1,2], their precise properties, however, are still under active investigation. An analogous (and even more perplexing) story applies to dark matter (DM) whose nature remains unknown despite the ever-growing evidence for its existence from the astrophysical observables. An intriguing possibility regarding these mysteries would be to introduce right-handed neutrinos (RHNs), which can address not only the neutrino mass and DM but also their potential roles in the inflation and baryon asymmetry production [3–9].

We, in this article, seek a possibility for a sterile RHN to make up the whole DM in the Universe and, in particular, propose the new production mechanism of sterile RHN DM through the mixing among RHNs. This is in contrast to the conventional mechanisms requiring the sterile RHN DM to couple to left-handed neutrinos which suffer from the severe tension between the bounds from the x-ray observation and the small-scale structure data [10–15]. These constraints, however, heavily depend on their production mechanisms and many possibilities have been explored to produce the desired DM abundance in addition to the conventional nonresonant/resonant active-sterile neutrino conversion mechanisms [6–9,16–20].

Our scenario is distinguishable from such alternative scenarios in that it still uses a simple oscillation between the thermal heavy RHN and DM, and yet it demonstrates the totally different features from the Dodelson-Widrow scenario such as the occurrence of the production peak above/around the electroweak which is of great advantage in circumventing the Lyman-α bounds due to the redshifting of DM momentum. After outlining our setup in Sec. II, we illustrate our scenario in Sec. III for a simple example of two RHNs. Section IV then demonstrates the concrete realization where we introduce a RHN mass matrix whose off-diagonal term can arise from the scalar field vacuum expectation value so that we can explain the light neutrino masses by the seesaw mechanism while avoiding the tight x-ray bounds. Section V is devoted to the discussion/conclusion.

II. SETUP

The Lagrangian we study is the standard model (SM) with three Majorana RHNs, given by $\mathcal{L} = \mathcal{L}_{\rm SM} + \mathcal{L}_N$ where $\mathcal{L}_{\rm SM}$ is the SM Lagrangian and $\mathcal{L}_N$ reads

$$\bar{\nu}_R i\partial\!\!\!/ \nu_R - \left[\nu_R^{cT} y_\nu L H - \frac{1}{2}\nu_R^{cT}\mathcal{M}_N \nu_R^c + \text{H.c.}\right], \qquad (1)$$

where H, L and ν_R are, respectively, the Higgs doublet, lepton doublet, and RHN. For simplicity, we concentrate on the case of three RHNs.

We begin with the field basis where $y_\nu y_\nu^\dagger$ is diagonal, denoted as $y_\nu^{\rm diag}$ so that $y_\nu^{\rm diag} y_\nu^{\rm diag\dagger}$ becomes a 3×3 diagonal matrix. $\mathcal{M}_N$ is, in general, a nondiagonal matrix, which we call the interaction basis. A familiar seesaw mechanism for the mass of left-handed neutrino ν_L reads, in terms of its Dirac mass $m_D^{\rm diag} = y_\nu^{\rm diag} v$ with $v = \langle H\rangle$, $\mathcal{M}_\nu = m_D^{{\rm diag}T}\mathcal{M}_N^{-1} m_D^{\rm diag}$ which can be

diagonalized as $\mathcal{M}_\nu^{\rm diag} = U_L^T \mathcal{M}_\nu U_L$ (U_L is the Pontecorvo-Maki-Nakagawa-Sakata matrix[1]). The neutrino mass eigenstates are

$$\begin{bmatrix} \nu_L \\ \nu_R^c \end{bmatrix} = U \begin{bmatrix} \nu \\ N^c \end{bmatrix}, \qquad U \simeq \begin{bmatrix} 1 & \theta^\dagger \\ -\theta & 1 \end{bmatrix} \begin{bmatrix} U_L & \\ & U_R^* \end{bmatrix}, \quad (2)$$

where $\theta \equiv \mathcal{M}_N^{-1} m_D^{\rm diag}$ and U_R is a unitary matrix defined to diagonalize $\mathcal{M}_N$ as $\mathcal{M}_N^{\rm diag} = U_R^\dagger \mathcal{M}_N U_R^*$. By taking the rotation of Eq. (2), the Yukawa coupling y_ν is in general a nondiagonal matrix while the neutrino masses, $\mathcal{M}_\nu$ and $\mathcal{M}_N$, are simultaneously diagonalized. We call this field basis the mass basis. Thus, we obtain

$$\begin{aligned} y_\nu^{\rm diag} y_\nu^{\rm diag\dagger} &= v^{-2} [U_R (\mathcal{M}_N^{\rm diag})^{1/2} R (\mathcal{M}_\nu^{\rm diag})^{1/2}] \\ &\times [U_R (\mathcal{M}_N^{\rm diag})^{1/2} R (\mathcal{M}_\nu^{\rm diag})^{1/2}]^\dagger, \end{aligned} \quad (3)$$

where R is an arbitrary 3×3 complex orthogonal matrix satisfying $R^T R = 1$ [21]. The mixing between ν_L and N is then parametrized by $\Theta = \theta^\dagger U_R^*$, and

$$\Theta^2 \equiv \Theta^\dagger \Theta = (\mathcal{M}_N^{\rm diag})^{-1/2} R \mathcal{M}_\nu^{\rm diag} R^\dagger (\mathcal{M}_N^{\rm diag})^{-1/2}. \quad (4)$$

The oscillations among RHNs can take place when their mass and interaction bases differ. We, in the following discussions, consider three RHNs with their masses $\mathcal{M}_N^{\rm diag} = {\rm diag}\{M_1, M_2, M_3\}$ and take N_1 as the lightest one so that it can play the role of DM. For the active neutrino masses, we parametrize $\mathcal{M}_\nu^{\rm diag} = {\rm diag}\{m_1, m_2, m_3\}$ for the normal hierarchy (NH), where $\Delta m_{21}^2 \equiv m_2^2 - m_1^2 = (7.50^{+0.19}_{-0.17}) \times 10^{-5}$ eV^2, $\Delta m_{31}^2 \equiv m_3^2 - m_1^2 = (2.457^{+0.047}_{-0.047}) \times 10^{-3}$ eV^2 [22]. For the inverted hierarchy (IH), we take $\mathcal{M}_\nu^{\rm diag} = {\rm diag}\{m_3, m_1, m_2\}$ and $\Delta m_{32}^2 \equiv m_3^2 - m_2^2 = (-2.449^{+0.048}_{-0.047}) \times 10^{-3}$ eV^2. The lightest neutrino mass (m_1 for the NH case, and m_3 for the IH case) is taken as a free parameter. In our discussions below, whenever it is not necessary to distinguish the mass orderings, m_1 refers to the lightest mass for brevity.

III. DM PRODUCTION THROUGH RHN OSCILLATION

We now check if enough abundance of RHN DM ν_{R1} can be produced from the RHN oscillations. In our scenario, the heavy RHNs ν_{R2} and ν_{R3} explain the left-handed neutrino masses by the seesaw mechanism and they can have sizable neutrino Yukawa couplings to be in the thermal equilibrium at a sufficiently high temperature. ν_{R1}, on the other hand, has a sufficiently small coupling to the SM species, so that its production is dominated by the conversion from heavier RHNs. For clarity of the following quantitative discussion, we focus on the ν_{R1} abundance produced only from its mixing with ν_{R2} because ν_{R3} plays the same role as ν_{R2} in producing ν_{R1}.

The relevant reactions for the ν_{R2} thermalization are the scatterings caused by Yukawa interaction, $\nu_{R2} L \leftrightarrow t Q_3$, $\nu_{R2} t \leftrightarrow L Q_3$, $\nu_{R2} Q_3 \leftrightarrow L t$, those involving the gauge bosons, $\nu_{R2} V \leftrightarrow H L$, $\nu_{R2} L \leftrightarrow H V$, $\nu_{R2} H \leftrightarrow L V$, and the decay and inverse decay $\nu_{R2} \leftrightarrow L H$ [$Q_3(t)$ is the left (right) handed top quark, and V represents the $SU(2)_L$ and $U(1)_Y$ gauge bosons].

The Boltzmann equation for ν_{R1} [23] reads

$$\frac{dn_{\nu_{R1}}}{dt} + 3Hn_{\nu_{R1}} = C_{\nu_{R1}} \quad (5)$$

where $C_{\nu_{R1}}$ represents the collision term integrated over the ν_{R1} momentum given by

$$C_{\nu_{R1}} \simeq \mathcal{P}(\nu_{R2} \to \nu_{R1})(\gamma_{\nu_{R2}}^{\rm col} + \gamma_{\nu_{R2}}^{\rm ID}), \quad (6)$$

$$\gamma_{\nu_{R2}}^{\rm col} = \frac{T}{64\pi^4} \int_{s_{\rm min}}^\infty ds \hat{\sigma} \sqrt{s} K_1(\sqrt{s}/T), \quad (7)$$

$$\gamma_{\nu_{R2}}^{\rm ID} = \frac{M_2^2 T}{\pi^2} \Gamma(\nu_{R2} \to LH) K_1(M_2/T). \quad (8)$$

Here $\mathcal{P}$ is the oscillation probability given by $\mathcal{P}(\nu_{R2} \to \nu_{R1}) = \frac{1}{2}\sin^2 2\theta_N$ (θ_N is the mixing angle between ν_{R1} and ν_{R2}), $\Gamma(\nu_{R2} \to LH) \simeq (y_\nu y_\nu^\dagger)_{22} M_2/(8\pi)$ is the decay width, and $\hat{\sigma}$ is the reduced cross section for the ν_{R2} collisions with the kinematical cut $s_{\rm min}$ of the Mandelstam variable s, and K_1 is the modified Bessel function of the first kind.[2]

ν_{R1} is efficiently produced when the collision terms are large.[3] Figure 1 shows Γ_i/H where Γ_i represents the rescaled reaction rates for the process i by taking the neutrino Yukawa coupling as unity (so that the curves can be easily scaled by multiplying the Yukawa coupling

[1]Throughout this article, we take the charged lepton Yukawa coupling to be diagonal.

[2]A factor $1/2$ in $\mathcal{P}$ comes from averaging out the RHN oscillation because the oscillation timescale is much shorter than the collision timescale involving ν_{R2}. More quantitatively, this averaging is justified for $T \lesssim 10^6$ GeV and/or $\Delta M^2 \equiv M_2^2 - M_1^2 \gtrsim 1$ GeV^2 because $t_{\rm osc}/t_{\rm col} \sim (y_\nu^2/10^{-14})(g^2/10^{-2})({\rm GeV}^2/\Delta M^2)(T/10^6\ {\rm GeV})^2$ where g represents a gauge coupling for a relevant gauge interaction. As we will discuss later, y_ν^2 of order 10^{-14} is required for GeV-scale RHN to reach the thermal equilibrium and it is automatically realized by enforcing the seesaw mechanism. The finite temperature effects on the RHN mixing angle θ_N are suppressed by the neutrino Yukawa couplings in our scenario and we simply consider a constant θ_N in our estimation. The cases when these approximations are not applicable are left for the future work.

[3]Some of collision terms, such as $\nu_R H \to L V$, possess the infrared divergences, which are regulated by the thermal mass of the propagator in our analysis for $T > T_C$ (T_C is the critical temperature of the electroweak phase transition and we take $T_C = 160$ GeV) [24–27].

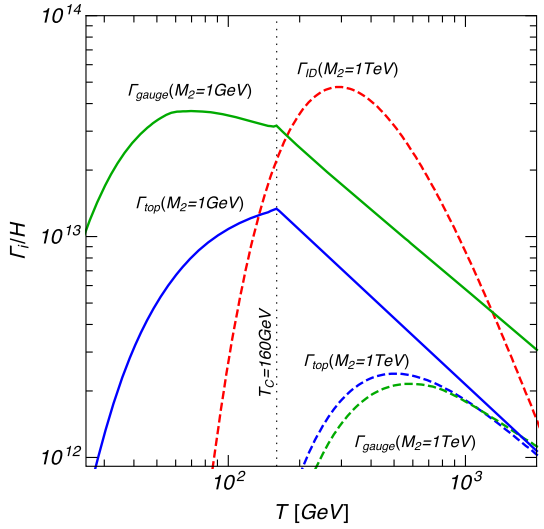

FIG. 1. The ratios between the rescaled (i.e., divided by the Yukawa couplings) reaction rates and the Hubble parameter are shown (the actual reaction rates are obtained by multiplying the Yukawa couplings). The solid curves are for $M_2 = 1$ GeV and the dashed curves are for $M_2 = 1$ TeV.

of interest). For illustration purpose, we define the reaction rates $\Gamma_i = \gamma^{\rm col}_{\nu_{R2}}(i)/n_\gamma$, where $n_\gamma = 2T^3/\pi^2$ is the radiation number density and $\gamma^{\rm col}_{\nu_{R2}}(i)$ are the collision terms involving the gauge bosons $[\gamma^{\rm col}_{\nu_{R2}}({\rm gauge})]$ and the top quarks $[\gamma^{\rm col}_{\nu_{R2}}({\rm top})]$. The inverse decay rate is given by $\Gamma_{\rm ID} = \gamma^{\rm ID}_{\nu_{R2}}/n_\gamma$. The figure shows the plots for $M_2 = 1$ GeV (solid) and for $M_2 = 1$ TeV (dashed), and we note that the inverse decay takes place only for the latter because of the kinematics, namely, the (inverse) decay is available only for $M_2 \gtrsim M_h$ with M_h being the Higgs mass. The actual reaction rates can be obtained by multiplying these rescaled reaction rates by $(y_\nu y_\nu^\dagger)_{22}$. We can see, from Fig. 1, that N_2 can reach the thermal equilibrium $(\Gamma_i/H \gtrsim 1)$ when $(y_\nu y_\nu^\dagger)_{22}$ is larger than $\mathcal{O}(10^{-13})$ for $M_2 = 1$–10^3 GeV, which is also in the desired numerical range to explain the neutrino masses by the seesaw mechanism.

The produced ν_{R1} (interaction state) constitutes the DM N_1 (mass eigenstate),[4] and the current N_1 relic number density can be estimated, in terms of the yield parameter $Y_{N_1} \equiv n_{N_1}/s$ (s is the entropy density), by integrating the Boltzmann equation from $T_{\rm RH}$, the reheating temperature, to the current temperature $T = T_0$

$$Y^0_{N_1} \equiv Y_{N_1}(T=0) = \int_0^\infty dT \mathcal{P}(\nu_{R2} \to \nu_{R1}) \frac{\gamma_{\nu_{R2}}}{sHT}, \quad (9)$$

[4]The produced ν_{R1} is composed of N_1 and N_2 which propagate with different velocities. As the ν_{R1} energy gets redshifted, these two mass states are eventually well separated and thus ν_{R1} is expected to mostly develop the N_1 component as long as $M_1 \ll M_2$, although the oscillation property may call for a careful study [28].

where we have taken the limits $T_{\rm RH} \to \infty$, $T_0 \to 0$, and $\gamma_{\nu_{R2}} \equiv \gamma^{\rm col}_{\nu_{R2}} + \gamma^{\rm ID}_{\nu_{R2}}$. The corresponding DM density can then be estimated in terms of the yield parameter

$$\Omega_{N_1} h^2 \simeq 0.12 \left[\frac{\sin^2 2\theta_N}{8.8\times 10^{-3}}\right]\left[\frac{|y_\nu^{\rm diag}|^2_{22}}{10^{-13}}\right]\left[\frac{M_1}{\rm keV}\right]\left[\frac{\tilde{Y}^0_{N_1}}{10^{12}}\right], \quad (10)$$

where $\tilde{Y}^0_{N_1}$ is the rescaled yield parameter, defined by factoring out the oscillation probability and the Yukawa coupling, $\tilde{Y}^0_{N_1} \equiv Y^0_{N_1}/(\mathcal{P}(\nu_{R2} \to \nu_{R1})(y_\nu y_\nu^\dagger)_{22})$. We found the following simple fitting formula to grasp the characteristic features of the DM abundance in our scenario

$$\log_{10}\tilde{Y}^0_{N_1} \simeq 12.8 \quad (M_2 \lesssim M_h)$$
$$\simeq 13.3 - (1/2)\log_{10}(M_2/M_h) \quad (M_2 \gtrsim M_h). \quad (11)$$

This behavior matches our expectation because, as emphasized in referring to Fig. 1, the most efficient production occurs when the production rate reaches maximal with respect to the Hubble expansion rate. $\tilde{Y}^0_{N_1}$ is hence little dependent on M_2 when M_2 is smaller than M_h, because N_2 is dominantly produced via the inverse decay in this case, and thus the temperature at which the production rate becomes maximal is at $T \simeq M_h$. For $M_2 \gtrsim M_h$, on the other hand, the SM particles possess the thermal mass and the production rate becomes maximal around $T \sim M_2$, which leads to some power dependence of the yield parameter on M_2. This is illustrated through a concrete example in the next section.

IV. BENCHMARK MODEL

We here discuss a possible realization of our scenario. Let us begin with a simple mass matrix given by

$$\mathcal{M}_N = \begin{bmatrix} M_0 & m & \\ m & M_2 & \\ & & M_3 \end{bmatrix}, \quad (12)$$

where m and M_0 are taken to be $M_0 \lesssim m \ll M_2, M_3$. $\mathcal{M}_N$ is then diagonalized as $\mathcal{M}_N^{\rm diag} = {\rm diag}\{M_1, M_2, M_3\}$ with $M_1 \simeq M_0 - m^2/M_2$ by using U_R, which reads

$$U_R^* \simeq \begin{bmatrix} 1 & \theta_N & \\ -\theta_N & 1 & \\ & & 1 \end{bmatrix}, \quad \theta_N = m/M_2. \quad (13)$$

The resultant N_1 abundance in the NH case is then given by

$$\Omega_{N_1} h^2 \simeq 0.12 \left[\frac{m_2}{0.01\ {\rm eV}}\right]\left[\frac{M_1}{\rm keV}\right]\left[\frac{(m/5\ {\rm GeV})^2}{M_2/100\ {\rm GeV}}\right]\left[\frac{\tilde{Y}^0_{N_1}}{10^{13}}\right], \quad (14)$$

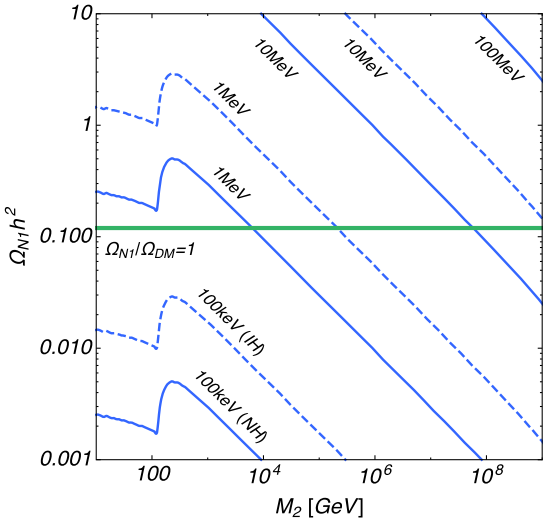

FIG. 2. The N_1 relic abundance is shown as a function of M_2 by varying M_1 from 100 keV to 100 MeV. The solid and dashed curves show the NH and IH cases, respectively.

while, in the IH case, m_2 should be replaced by m_1. In the case of $M_0 \ll m^2/M_2$, we can take $\theta_N \simeq (M_1/M_2)^{1/2}$ due to $M_1 \simeq m^2/M_2$, and thus we obtain

$$\Omega_{N_1}h^2 \simeq 0.12\left[\frac{m_2}{0.01\ \text{eV}}\right]\left[\frac{M_1}{0.52\ \text{MeV}}\right]^2\left[\frac{\tilde{Y}^0_{N_1}}{10^{13}}\right]. \quad (15)$$

For this simplified case, Fig. 2 shows $\Omega_{N_1}h^2$ as a function of M_2 for various M_1 taken from 100 keV to 100 MeV in both the NH and IH cases, which are depicted by solid and dashed curves, respectively.[5] The green band in the figure indicates the observed value of the DM abundance given by $\Omega_{\rm DM}h^2 = 0.1197 \pm 0.0022$ [29].

On the other hand, since Θ^2_{11} depends on θ_N and we need a relatively large θ_N for our scenario to work, the N_1 is subject to the x-ray constraint given by $\Theta^2_{11} \lesssim 10^{-5}(\text{keV}/M_1)^5$ [12]. One may simply expect that the x-ray bound is easily circumvented because the Yukawa coupling of ν_{R1} can be negligibly small. We, however, point out that the light RHN can decay into the SM particles through its oscillation to a heavier RHN. In our current setup, we obtain $\Theta^2_{11} = M_1^{-1}(m_1|R_{11}|^2 + m_2|R_{12}|^2 + m_3|R_{13}|^2)$, where R_{ij} represents the (i,j) entry of the R matrix. We can now take $R_{13} = 0$, since there is no mixing in this component, and $m_1 = 0$ is experimentally allowed. However, since we have $|R_{12}|^2 = 1/(1 + (M_1/M_2)\cot^2\theta_N) \sim 1/2$ in our setup with $M_1/M_2 \ll 1$, large M_1 is not allowed because of the x-ray constraint $\Theta^2_{11} \simeq m_2/(2M_1) \lesssim 10^{-5}(\text{keV}/M_1)^5$, where $m_2 \simeq \sqrt{\Delta m^2_{21}}$ in the NH case, and m_2 is replaced by $m_1 \simeq \sqrt{|\Delta m^2_{32}|}$ in the IH case. One may naively expect that this decay of light RHN through a heavier RHN is suppressed by the hierarchically large mass ratio $M_1/M_2 \ll 1$. If we did not enforce the simple seesaw mechanism to obtain the desirable light neutrino masses, this would be the case and the x-ray bound could be circumvented. We, however, in our model construction, stick to the seesaw mechanism to account for the observed neutrino masses, which then inevitably increase y_2 if we choose a bigger value of M_2 to result in too big an x-ray decay rate. To keep the virtue of explaining the observed neutrino masses by the simple type-I seesaw mechanism and yet not to lose the attractive feature of simple RHN oscillation production, we now discuss a time-dependent RHN mixing to evade the x-ray constraint mentioned above.

Such a time-dependent RHN mixing can be achieved by utilizing the dynamics of a real scalar filed ϕ. Let us here consider the two flavor case for simplicity, but the extension to the three flavor system is straightforward. In the two flavor case, we impose Z_2 symmetry under which ν_{R2} is even, while ν_{R1} and ϕ are odd.[6] Now the mass matrix $\mathcal{M}_N$ in Eq. (1) is given by

$$\mathcal{M}_N(\phi) = \begin{bmatrix} M_1 & \kappa\phi \\ \kappa\phi & M_2 \end{bmatrix} \quad (16)$$

in the interaction basis. The dynamics of ϕ is governed by the equation of motion $\ddot{\phi} + 3H\dot{\phi} + V'(\phi) = 0$, where $V(\phi)$ is the potential that we take $V(\phi) \simeq (1/2)m^2_\phi\phi^2$. For $m_\phi \ll 3H$, ϕ is almost constant, namely, $\phi \simeq \sqrt{2\rho_\phi}/m_\phi$ with ρ_ϕ the energy density of ϕ, and when H drops below m_ϕ, ϕ starts to oscillate. As we will see below, $m_\phi \ll 3H$ is always satisfied when the N_1 production rate is maximal, and thus we take ϕ as a constant in this regime.

The mixing angle between ν_{R1} and ν_{R2} is given by $\sin\theta_N \simeq \kappa\phi/M_2$ in the case that $M_1 \ll M_2$, and thus in the constant ϕ regime we obtain $\sin^2 2\theta_N \simeq 4\kappa^2\rho_\phi/(m^2_\phi M^2_2)$, where the relevant θ_N is determined by $\rho_\phi(T_{\rm max})$ with $T_{\rm max}$ being the temperature at which the production rate becomes maximal, namely, $T_{\rm max} \sim T_c$ for $M_2 \lesssim T_c$ and otherwise $T_{\rm max} \sim M_2$. As mentioned above, ϕ is constant until it starts to oscillate, so we can take $\rho_\phi(T_{\rm max}) \simeq \rho_\phi(T_{\rm osc})$ with $T_{\rm osc}$ given by $m_\phi = 3H(T_{\rm osc})$. Then, we obtain

$$\sin^2 2\theta_N \simeq 0.3 \times \left[\frac{r_g}{30}\right]^{1/4}\left[\frac{\kappa}{10^{-9}}\right]^2\left[\frac{m_\phi}{10^{-4}\ \text{eV}}\right]^{-1/2} \times \left[\frac{M_2}{100\ \text{GeV}}\right]^{-2}\left[\frac{r}{10^{-4}}\right], \quad (17)$$

[5]It should be noted that, in Fig. 2, $t_{\rm osc}/t_{\rm col} \ll 1$ is achieved for $T \lesssim 10^6 \times M_2$ even in the large M_2 region, so that a factor $1/2$ in $\mathcal{P}$ by averaging out the RHN oscillation is justified.

[6]Although our setup is similar to the idea discussed in Ref. [30], the DM production scenario is quite different, since our scenario does not rely on the oscillation between active and sterile neutrinos, and thus the temperature at which the production efficiently occurs takes rather a wide range, which can imprint an observable signature on the structure formation.

with $r_g = g_*(T_{\rm osc})/g_*(T_0)$, and $r = \rho_\phi^0/\rho_{\rm DM}$ with ρ_ϕ^0 and $\rho_{\rm DM}$ being the energy density of ϕ and dark matter at the present. Here we have used $g_*(T_0) \simeq 3.36$.

We also require that ϕ never thermalizes by taking a sufficiently small κ not to affect the big bang nucleosynthesis, which results in $\kappa^2 \lesssim M_2/M_{\rm Pl}$. In addition, m_ϕ should be smaller than $H(T_{\rm max})$ in order for ϕ at $T_{\rm max}$ to be constant, where $H(T_{\rm max}) \simeq 10^{-5}$ eV for $M_2 < T_c$ and $H(T_{\rm max}) \simeq 10^{-5} \times (M_2/T_c)^2$ for $M_2 > T_c$.

It is worth mentioning that the dynamics of ϕ may be tied to inflationary models. In particular, the condition of $\rho_\phi^0 \ll \rho_{\rm DM}$ implies that the initial amplitude of ϕ is bounded

$$\phi \lesssim 4 \times 10^{11}\ {\rm GeV} \left(\frac{r_g}{30}\right)^{1/2} \left(\frac{r}{10^{-4}}\right)^{1/2} \left(\frac{10^{-4}\ {\rm eV}}{m_\phi}\right)^{1/4}. \quad (18)$$

On the other hand, ϕ could be largely displaced from the origin during inflation and its oscillation at a later time possibly dominates the dark matter energy density, in an analogous manner to the Polonyi/moduli problem [31–33]. To suppress ϕ in our case, we may utilize a relatively strong coupling between ϕ and inflaton, which renders the adiabatic suppression of the amplitude of the coherent oscillations [34]. Its actual dynamics, however, depends on the inflationary models and how ϕ couples to the inflaton, which we leave unspecified for the future work.

Finally, let us comment on the θ_N at the present, which is relevant for the decay of N_1. Below $T_{\rm osc}$, since ρ_ϕ drops as a matter energy density, we obtain

$$\frac{\sin^2 2\theta_N(T_0)}{\sin^2 2\theta_N(T_{\rm osc})} \simeq 1.2 \times 10^{-46} \left[\frac{r_g}{30}\right]^{-1/4} \left[\frac{m_\phi}{10^{-4}\ {\rm eV}}\right]^{-3/2}, \quad (19)$$

and therefore a sufficiently small mixing to avoid the x-ray constraint can be achieved.

V. DISCUSSION/CONCLUSION

Before concluding our discussions, let us briefly point out another potentially interesting production mechanism: the production of N_1 from a heavier RHN decay. We can consider the decay of N_2 (and/or N_3) which is thermally decoupled while it is relativistic (otherwise N_2 number density would be too small due to the Boltzmann suppression). N_1 abundance then can be estimated as

$$\Omega_{N_1} h^2 \simeq 10^{-10} \left[\frac{\Theta_{11}^2}{10^{-12}}\right] \left[\frac{M_1}{10\ {\rm keV}}\right] \left[\frac{g_*(T_0)}{g_*(T_{\rm FO})}\right] \quad (20)$$

where we used the branching fraction of N_2 decay for the process $N_2 \to N_1 + ({\rm mesons, leptons})$, ${\rm Br}(N_2 \to N_1) \simeq \Gamma(N_2 \to N_1)/\Gamma(N_2 \to SM) \simeq M_2 \Theta_{11}^2 \Theta_{22}^2 / M_2 \Theta_{22}^2 \simeq \Theta_{11}^2$, and the ratio of g_* accounts for the change in the effective degrees of freedom from the N_2 freeze-out epoch to the present time. This production contribution is hence subdominant compared with RHN oscillation production in the parameter region of our interest.

Let us next mention the small-scale structure constraints applicable to our scenario. We here discuss the Lyman-α forest constraints which can give the lower limit on the DM mass from the DM free streaming scale $\lambda_{\rm FS} \sim 1\ {\rm Mpc}({\rm keV}/M_1)(\langle p/T \rangle/3.15)$ [35]. Too large a free streaming scale can be excluded due to the suppression of small-scale structure formation. The average momentum of N_1 produced by the nonresonant oscillation of thermalized N_2 can be estimated as $\langle p_1 \rangle \sim 2.8T$, analogous to the conventional (nonresonant) active-sterile oscillation scenario. Taking account of momentum redshifting by a factor $(g_*(T_{N_2 \to N_1})/g_*(T \ll {\rm MeV}))^{-1/3}$ due to the change in the effective degrees of freedom, Lyman-α data leads to the RHN DM mass bound $M_1 \gtrsim 10$ keV for our scenario [14] (when $N_2 \to N_1$ occurs most efficiently before the QCD phase transition, which is the case for the parameter range discussed so far). Such a DM mass range can be realized in our scenario as explicitly demonstrated through the concrete examples in the last section while being compatible with both the right relic abundance and seesaw mechanism.

Among the possible extensions of our DM scenarios, we plan to study the leptogenesis as well as the neutrino observables such as the neutrinoless double beta decay in our future work. For instance, even though we have focused on the DM production in this article, the neutrino Yukawa couplings in our model can be further constrained by seeking the production of desirable baryon asymmetry in the Universe. The realization of leptogenesis when N_2 and N_3 are heavy enough and/or are degenerate in their masses with sufficient CP violations [5,6,24] will be explored in our forthcoming paper. The CP phases in the neutrino Yukawa couplings are of great importance not only for the leptogenesis but also for the DM production in our scenario, and the presented production mechanism for the RHN DM could uncover a new connection between DM and leptogenesis to bring considerable opportunities for subsequent studies.

ACKNOWLEDGMENTS

This work was supported by Institute for Basic Science (IBS) under the project code IBS-R018-D1. We thank A. Kamada, A. Merle, and T. Asaka for useful discussions and, in particular, the anonymous referee for the constructive suggestions.

[1] Y. Fukuda *et al.* (Super-Kamiokande Collaboration), Evidence for Oscillation of Atmospheric Neutrinos, Phys. Rev. Lett. **81**, 1562 (1998).

[2] Q. R. Ahmad *et al.* (SNO Collaboration), Direct Evidence for Neutrino Flavor Transformation from Neutral Current Interactions in the Sudbury Neutrino Observatory, Phys. Rev. Lett. **89**, 011301 (2002).

[3] T. Yanagida, Horizontal symmetry and masses of neutrinos, in *Proceedings of the Workshop on Unified Theory and Baryon Number of the Universe*, edited by O. Sawada and A. Sugamoto [*Conf. Proc.* C7902131, p. 95–99 (1979)] ; M. Gell-Mann, P. Ramond, and R. Slansky, in *Supergravity*, edited by P. van Niewwenhuizen and D. Freedman (North Holland, Amsterdam, 1979); S. L. Glashow, in *Quarks and Leptons, Cargèse 1979*, edited by M. Lévy *et al.* (Plenum, New York, 1980), p. 707.See also P. Minkowski, $\mu \to e\gamma$ at a rate of one out of 1-billion muon decays?, Phys. Lett. B **67**, 421 (1977).

[4] T. Asaka, S. Blanchet, and M. Shaposhnikov, The nuMSM, dark matter and neutrino masses, Phys. Lett. B **631**, 151 (2005).

[5] M. Fukugita and T. Yanagida, Baryogenesis without grand unification, Phys. Lett. B **174**, 45 (1986).

[6] T. Asaka and M. Shaposhnikov, The nuMSM, dark matter and baryon asymmetry of the universe, Phys. Lett. B **620**, 17 (2005).

[7] L. Canetti, M. Drewes, T. Frossard, and M. Shaposhnikov, Dark matter, baryogenesis and neutrino oscillations from right-handed neutrinos, Phys. Rev. D **87**, 093006 (2013).

[8] M. Ibe and K. Kaneta, Spontaneous thermal leptogenesis via Majoron oscillation, Phys. Rev. D **92**, 035019 (2015).

[9] H. Murayama, H. Suzuki, T. Yanagida, and J. Yokoyama, Chaotic inflation and baryogenesis in supergravity, Phys. Rev. D **50**, R2356 (1994); J. R. Ellis, M. Raidal, and T. Yanagida, Sneutrino inflation in the light of WMAP: Reheating, leptogenesis and flavor violating lepton decays, Phys. Lett. B **581**, 9 (2004); K. Kadota and J. Yokoyama, D-term inflation and leptogenesis by right-handed sneutrino, Phys. Rev. D **73**, 043507 (2006).

[10] S. Dodelson and L. M. Widrow, Sterile-Neutrinos as Dark Matter, Phys. Rev. Lett. **72**, 17 (1994).

[11] S. Tremaine and J. E. Gunn, Dynamical Role of Light Neutral Leptons in Cosmology, Phys. Rev. Lett. **42**, 407 (1979).

[12] A. Boyarsky, A. Neronov, O. Ruchayskiy, and M. Shaposhnikov, Constraints on sterile neutrino as a dark matter candidate from the diffuse x-ray background, Mon. Not. R. Astron. Soc. **370**, 213 (2006).

[13] S. Horiuchi, P. J. Humphrey, J. Onorbe, K. N. Abazajian, M. Kaplinghat, and S. Garrison-Kimmel, Sterile neutrino dark matter bounds from galaxies of the local group, Phys. Rev. D **89**, 025017 (2014); K. Perez, K. C. Y. Ng, J. F. Beacom, C. Hersh, S. Horiuchi, and R. Krivonos, (Almost) closing the νMSM sterile neutrino dark matter window with NuSTAR, Phys. Rev. D **95**, 123002 (2017); J. F. Cherry and S. Horiuchi, Closing in on resonantly produced sterile neutrino dark matter, Phys. Rev. D **95**, 083015 (2017).

[14] V. Iri *et al.*, New constraints on the free-streaming of warm dark matter from intermediate and small scale Lyman-α forest data, Phys. Rev. D **96**, 023522 (2017).

[15] X. D. Shi and G. M. Fuller, New Dark Matter Candidate: Nonthermal Sterile Neutrinos, Phys. Rev. Lett. **82**, 2832 (1999).

[16] T. Asaka, M. Shaposhnikov, and A. Kusenko, Opening a new window for warm dark matter, Phys. Lett. B **638**, 401 (2006); M. Shaposhnikov and I. Tkachev, The nuMSM, inflation, and dark matter, Phys. Lett. B **639**, 414 (2006); A. Kusenko, Sterile Neutrinos, Dark Matter, and Pulsar Velocities in Models with a Higgs Singlet, Phys. Rev. Lett. **97**, 241301 (2006); K. Petraki and A. Kusenko, Dark-matter sterile neutrinos in models with a gauge singlet in the Higgs sector, Phys. Rev. D **77**, 065014 (2008); H. Matsui and M. Nojiri, Higgs sector extension of the neutrino minimal standard model with thermal freeze-in production mechanism, Phys. Rev. D **92**, 025045 (2015); A. Merle, V. Niro, and D. Schmidt, New production mechanism for keV sterile neutrino dark matter by decays of frozen-in scalars, J. Cosmol. Astropart. Phys. 03 (2014) 028; Z. Kang, Upgrading sterile neutrino dark matter to FI*m*P using scale invariance, Eur. Phys. J. C **75**, 471 (2015); S. B. Roland, B. Shakya, and J. D. Wells, Neutrino masses and sterile neutrino dark matter from the PeV scale, Phys. Rev. D **92**, 113009 (2015); A. Merle and M. Totzauer, keV sterile neutrino dark matter from singlet scalar decays: Basic concepts and subtle features, J. Cosmol. Astropart. Phys. 06 (2015) 011; Z. Kang, View FImP miracle (by scale invariance) à la self-interaction, Phys. Lett. B **751**, 201 (2015); A. Adulpravitchai and M. A. Schmidt, Sterile neutrino dark matter production in the Neutrino-phillic two Higgs doublet model, J. High Energy Phys. 12 (2015) 1; M. Drewes and J. U. Kang, Sterile neutrino dark matter production from scalar decay in a thermal bath, J. High Energy Phys. 05 (2016) 051.

[17] F. Bezrukov, H. Hettmansperger, and M. Lindner, keV sterile neutrino Dark Matter in gauge extensions of the standard model, Phys. Rev. D **81**, 085032 (2010); M. Nemevsek, G. Senjanovic, and Y. Zhang, Warm dark matter in low scale left-right theory, J. Cosmol. Astropart. Phys. 07 (2012) 006; K. Kaneta, Z. Kang, and H. S. Lee, Right-handed neutrino dark matter under the B-L gauge interaction, J. High Energy Phys. 02 (2017) 031.

[18] K. Kadota, Sterile neutrino dark matter in warped extra dimensions, Phys. Rev. D **77**, 063509 (2008); A. V. Patwardhan, G. M. Fuller, C. T. Kishimoto, and A. Kusenko, Diluted equilibrium sterile neutrino dark matter, Phys. Rev. D **92**, 103509 (2015); A. Merle, A. Schneider, and M. Totzauer, Dodelson-Widrow production of sterile neutrino dark matter with nontrivial initial abundance, J. Cosmol. Astropart. Phys. 04 (2016) 003.

[19] A. Anisimov and P. Di Bari, Cold dark matter from heavy right-handed neutrino mixing, Phys. Rev. D **80**, 073017 (2009); P. Di Bari, P. O. Ludl, and S. Palomares-Ruiz, Unifying leptogenesis, dark matter and high-energy neutrinos with right-handed neutrino mixing via Higgs portal, J. Cosmol. Astropart. Phys. 11 (2016) 044.

[20] M. Drewes *et al.*, A white paper on keV sterile neutrino dark matter, J. Cosmol. Astropart. Phys. 01 (2017) 025.

[21] J. A. Casas and A. Ibarra, Oscillating neutrinos and $\mu \to e$, γ, Nucl. Phys. **B618**, 171 (2001); A. Broncano,

M. B. Gavela, and E. E. Jenkins, The effective Lagrangian for the seesaw model of neutrino mass and leptogenesis, Phys. Lett. B **552**, 177 (2003); The effective Lagrangian for the seesaw model of neutrino mass and leptogenesis, Phys. Lett. B **636**, 332(E) (2006); J. A. Casas, A. Ibarra, and F. Jimenez-Alburquerque, Hints on the high-energy seesaw mechanism from the low-energy neutrino spectrum, J. High Energy Phys. 04 (2007) 064; M. Blennow and E. Fernandez-Martinez, Parametrization of seesaw models and light sterile neutrinos, Phys. Lett. B **704**, 223 (2011); J. Heeck, Seesaw parametrization for n right-handed neutrinos, Phys. Rev. D **86**, 093023 (2012).

[22] M. C. Gonzalez-Garcia, M. Maltoni, and T. Schwetz, Global analyses of neutrino oscillation experiments, Nucl. Phys. **B908**, 199 (2016).

[23] A. D. Dolgov and S. H. Hansen, Massive sterile neutrinos as warm dark matter, Astropart. Phys. **16**, 339 (2002).

[24] A. Pilaftsis and T. E. J. Underwood, Resonant leptogenesis, Nucl. Phys. **B692**, 303 (2004).

[25] D. Besak and D. Bodeker, Thermal production of ultrarelativistic right-handed neutrinos: Complete leading-order results, J. Cosmol. Astropart. Phys. 03 (2012) 029.

[26] M. D'Onofrio, K. Rummukainen, and A. Tranberg, Sphaleron Rate in the Minimal Standard Model, Phys. Rev. Lett. **113**, 141602 (2014).

[27] M. D'Onofrio and K. Rummukainen, Standard model crossover on the lattice, Phys. Rev. D **93**, 025003 (2016).

[28] E. Akhmedov, D. Hernandez, and A. Smirnov, Neutrino production coherence and oscillation experiments, J. High Energy Phys. 04 (2012) 052.

[29] P. A. R. Ade *et al.* (Planck Collaboration), Planck 2015 results. XIII. Cosmological parameters, Astron. Astrophys. **594**, A13 (2016).

[30] A. Berlin and D. Hooper, Axion-assisted production of sterile neutrino dark matter, Phys. Rev. D **95**, 075017 (2017).

[31] G. D. Coughlan, W. Fischler, E. W. Kolb, S. Raby, and G. G. Ross, Cosmological problems for the polonyi potential, Phys. Lett. **131B**, 59 (1983).

[32] J. R. Ellis, D. V. Nanopoulos, and M. Quiros, On the axion, dilaton, polonyi, gravitino and shadow matter problems in supergravity and superstring models, Phys. Lett. B **174**, 176 (1986).

[33] A. S. Goncharov, A. D. Linde, and M. I. Vysotsky, Cosmological problems for spontaneously broken supergravity, Phys. Lett. **147B**, 279 (1984).

[34] A. D. Linde, Relaxing the cosmological moduli problem, Phys. Rev. D **53**, R4129 (1996).

[35] K. Abazajian, G. M. Fuller, and M. Patel, Sterile neutrino hot, warm, and cold dark matter, Phys. Rev. D **64**, 023501 (2001).